Two-body and three-body spin substructures serve as building blocks in small spin-3 condensates

C. G. Bao*

Center of Theoretical Nuclear Physics, National Laboratory of Heavy Ion Accelerator, Lanzhou, 730000, People's Republic of China and State Key Laboratory of Optoelectronic Materials and Technologies, School of Physics and Engineering, Sun Yat-Sen University, Guangzhou, 510275, People's Republic of China

(Received 23 November 2011; published 19 April 2012)

It is found that stable few-body spin structures, pairs and triplexes in the spin space, may exist as basic constituents in small spin-3 condensates, and they play the role of building blocks when the parameters of interaction fall in particular domains. A specific method is designed to find these constituents.

DOI: 10.1103/PhysRevA.85.043616 PACS number(s): 03.75.Hh, 03.75.Mn, 75.10.Jm, 05.30.Jp

I. INTRODUCTION

When the structure of a few-body fermion system is very stable, it may become a basic constituent of many-body systems. For an example, the structures of light nuclei can be explained based on the cluster model, where the α particle is the building block [1,2]. Another famous example is the Cooper pair in condensed matter [3,4]. This pair is responsible for superconductivity. For boson systems, the situation is a little different because all the particles might have the same spatial wave function. However, the existence of basic spin substructures in spin space is possible. For Bose-Einstein condensates of spin-1 and spin-2 atoms, basic few-body substructures have already been proposed by theorists. For spin-1 condensates, the interaction can be written as

$$V_{ij} = \delta(\boldsymbol{r_i} - \boldsymbol{r_j}) \sum_S g_S \mathcal{P}_S, \tag{1}$$

where S is the combined spin of i and j and has two possible values, 0 or 2. $\mathcal{P}_S$ is the projector of the S channel, and g_S is the strength proportional to the s-wave scattering length of the S channel. When $g_2 - g_0$ is positive, the ground state will have total spin $F = 0$ (1) when the particle number N is even (odd) [5–8]. The ground-state wave function Ψ_g is proportional to the pair state $\tilde{P}_N[(\varsigma\varsigma)_0]^{N/2}$ or $\tilde{P}_N\varsigma[(\varsigma\varsigma)_0]^{(N-1)/2}$, where ς denotes the spin state of a spin-1 atom, a pair of them are coupled to zero, and $\tilde{P}_N$ is the symmetrizer (simply a summation over the $N!$ permutation terms). For higher states, say, the one with $F = 2$, the total spin state is proportional to $\tilde{P}_N(\varsigma\varsigma)_2[(\varsigma\varsigma)_0]^{(N-2)/2}$. Thus, the singlet pair $(\varsigma\varsigma)_0$ appears as a common building block in the spin space. These pairs, together with a few other substructures, constitute all the low-lying states.

For spin-2 condensates, the interaction can also be written as Eq. (1), but with $S = 0, 2$, and 4. A detailed classification of the spin states based on the seniority and the total spin F was given in Ref. [7]. When N is even and $\frac{7}{10}(g_0 - g_4) < (g_2 - g_4) < -\frac{7(N+3)}{10(N-2)}(g_0 - g_4)$, Ψ_g is also dominated by the singlet pairs and is proportional to the pair state $\tilde{P}_N[(\eta\eta)_0]^{N/2}$, where η denotes the spin state of a spin-2 atom. When N is a multiple of 3 and $(g_2 - g_4)$ is negative and smaller than $\frac{7}{10}(g_0 - g_4)$, Ψ_g is nearly proportional to the triplex state $\tilde{P}_N[((\eta\eta)_2\eta)_0]^{N/3}$. Obviously, the triplex $((\eta\eta)_2\eta)_0$ acts as a building block in the spin space. Furthermore, when the parameters of interaction fall inside the indicated domain, the low-lying states are also dominated by these building blocks, accompanied by a few other substructures.

It is evident that the existence of building blocks originates from special features of the interaction. The pairs $(\varsigma\varsigma)_S$ and $(\eta\eta)_S$ may appear as building blocks whenever g_S is sufficiently negative. For spin-f atoms with f even, instead of the pairs, a more favorable substructure might be a triplex as shown above with $f = 2$. Let ϑ denote the spin state of a spin-f particle. For the triplex state $\tilde{P}_N((\vartheta\vartheta)_f\vartheta)_\lambda$, the symmetrizer $\tilde{P}_N$ is not necessary when $\lambda = 0$ because $((\vartheta\vartheta)_f\vartheta)_0$ itself is symmetric [i.e., $((\vartheta(i)\vartheta(j))_f\vartheta(k))_0 = ((\vartheta(j)\vartheta(k))_f\vartheta(i))_0$ as can be verified by recoupling the spins]. This implies that every two spins are coupled to f. Thereby the binding will be maximized if g_f is sufficiently negative. Intuitively speaking, the relative orientations of the three spins in the $\lambda = 0$ triplex are shown in Fig. 1(b), where the angles between every two spins are 120° to assure that they are coupled to f. Therefore, for spin-f condensates, one can predict that the $\lambda = 0$ triplexes will serve as building blocks in spin space when g_f is sufficiently negative (note that the $\lambda = 0$ triplex is prohibited when f is odd).

The ground-state structure of spin-3 condensates has already been studied based on the mean-field theory (MFT) [9–11]. In this theory the spin structure is described by the phases of spinors. They will have the polar phase (corresponding to the pair state) when g_0 is sufficiently negative and have the cyclic phase (corresponding to the triplex state) when g_0 becomes positive. If a magnetic field is applied, a number of phases will emerge. Instead of using the spinors and going beyond the MFT, in this paper we attempt to describe the spin structures based on the basic constituents. From the experience with spin-1 and -2 condensates, it is expected that pairs and triplexes might also appear in spin-3 condensates when the parameters of interaction are appropriate. We are going to search for these basic constituents. Due to the difficulty in calculation, only small condensates (N is small) are concerned. We believe that the knowledge from small systems will help us to understand better the larger systems. Due to the prohibition of the $\lambda = 0$ triplex, only $\lambda \neq 0$ triplexes could emerge in spin-3 systems. Since each λ triplex has $2\lambda + 1$ magnetic components, additional complexity will arise as shown below.

*stsbcg@mail.sysu.edu.cn

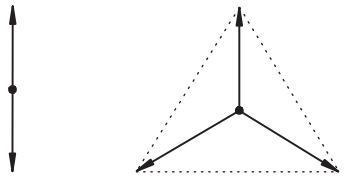

FIG. 1. Basic constituents of condensates in spin space: the pair (a) and triplex (b). In these diagrams the spatial locations of the spins are not meaningful, only their relative orientations.

II. HAMILTONIAN, EIGENSTATES, AND PARTICLE CORRELATION

Let N spin-3 atoms be confined by an isotropic and parabolic trap with frequency ω. The interaction between particles i and j is $V_{ij} = \delta(\boldsymbol{r_i} - \boldsymbol{r_j}) \sum_S g_S \mathcal{P}_S + V_{\rm dd}$, where $V_{\rm dd}$ is the dipole-dipole interaction. Let the wave function for the relative motion of i and j be ψ_{lSJ}, where l is the relative orbital angular momentum, and l and S are coupled to J. Then, for $l = 0$, the matrix element $\langle \psi_{l'S'J}|V_{\rm dd}|\psi_{0SJ}\rangle$ is nonzero only if $l' = 2$. This implies that $V_{\rm dd}$ will play its role only if accompanied by a d-wave spatial excitation. It is assumed that ω is so large that $\langle \psi_{2S'J}|V_{\rm dd}|\psi_{0SJ}\rangle \ll 2\hbar\omega$. In this case the effect of $V_{\rm dd}$ is suppressed so that it can be neglected. Note that, in general, $V_{\rm dd}$ will be important in spin evolution where higher partial waves emerge. However, this is not the case for an equilibrium state in a strong isotropic trap at very low temperature [10–12]. Furthermore, we consider a small condensate so that the size of the condensate is smaller than the spin healing length. In this case the single-spatial-mode approximation (SMA) is reasonable and is therefore adopted [13].

Let the common spatial wave function be $\phi(\boldsymbol{r})$. Under the SMA, after integration over the spatial degrees of freedom, we arrive at a model Hamiltonian

$$H_{\rm mod} = \sum_{i<j} V'_{ij}, \tag{2}$$

where $V'_{ij} = \sum_S G_S \mathcal{P}_S$, $G_S = g_S \int |\phi(\boldsymbol{r})|^4 d\boldsymbol{r}$.

For diagonalizing $H_{\rm mod}$, the set of normalized and symmetrized Fock states

$$\begin{aligned}|\alpha\rangle &= \left|N_3^\alpha, N_2^\alpha, N_1^\alpha, N_0^\alpha, N_{-1}^\alpha, N_{-2}^\alpha, N_{-3}^\alpha\right\rangle \\ &\equiv \frac{1}{\sqrt{N! N_3^\alpha! \cdots N_{-3}^\alpha!}} \\ &\quad \times \tilde{P}_N \left\{ \prod_{i_3} \chi_3(i_3) \prod_{i_2} \chi_2(i_2) \cdots \prod_{i_{-3}} \chi_{-3}(i_{-3}) \right\}\end{aligned} \tag{3}$$

are used as basis functions, where $\chi_\mu(i)$ is the spin state of the ith particle in component μ (from 3 to -3), i_μ runs from 1 to N_μ^α, and N_μ^α is the number of particles in μ, $\sum_\mu N_\mu^\alpha = N$, and $\sum_\mu \mu N_\mu^\alpha = M$, where M is the magnetization. Incidentally, the creation and annihilation operators of bosons are not used in this paper. Since the $|\alpha\rangle$'s as a whole form a complete set, once the matrix elements $\langle \alpha'|H_{\rm mod}|\alpha\rangle$ have been calculated, exact eigenenergies and eigenstates of $H_{\rm mod}$ can be obtained via diagonalization (the details are referred to [14]). Obviously, both the total spin F and its Z component M are conserved when $V_{\rm dd}$ is neglected.

Let the ith eigenstate be denoted as ψ_i with total spin $F(i)$ and magnetization $M(i)$. The state can be expanded as $\psi_i = \sum_\alpha c_\alpha |\alpha\rangle$. Since one can extract a particle from a Fock state, one can also extract a particle from ψ_i via the expansion as

$$\begin{aligned}\psi_i &\equiv \sum_\mu \chi_\mu(1) \psi_\mu^i, \\ \psi_\mu^i &= \sum_\alpha c_\alpha \sqrt{\frac{N_\mu^\alpha}{N}} \left|\cdots, N_\mu^\alpha - 1, \cdots\right\rangle.\end{aligned} \tag{4}$$

With Eq. (4), we know that the probability of a particle being in μ is just

$$P_\mu^i \equiv \langle \psi_\mu^i | \psi_\mu^i \rangle. \tag{5}$$

The probabilities fulfill $\sum_\mu P_\mu^i = 1$. P_μ^i is called the one-body probability, and $N P_\mu^i$ is just the average population of the μ component.

If one more particle is further extracted, in a similar way, we have

$$\psi_i = \sum_{\mu,\nu} \chi_\mu(1) \chi_\nu(2) \varphi_{\mu\nu}^i. \tag{6}$$

We define

$$P_{\mu\nu}^i \equiv \langle \varphi_{\mu\nu}^i | \varphi_{\mu\nu}^i \rangle. \tag{7}$$

These probabilities fulfill $P_{\mu\nu}^i = P_{\nu\mu}^i$, $\sum_{\mu\nu} P_{\mu\nu}^i = 1$, and $\sum_\nu P_{\mu\nu}^i = P_\mu^i$. When two particles are observed simultaneously, obviously the probability of one being in μ and the other one in ν is $P_{\mu\nu}^i + P_{\nu\mu}^i$ (if $\mu \neq \nu$) or $P_{\mu\mu}^i$ (if $\mu = \nu$). $P_{\mu\nu}^i$ is called the correlative probability of spin components.

Let Eq. (6) be rewritten as

$$\psi_i = \sum_{S,m_S} [\chi(1)\chi(2)]_{S,m_S} \sum_\mu C_{3,\mu,3,m_S-\mu}^{S,m_S} \varphi_{\mu,m_S-\mu}^i. \tag{8}$$

Then, the probability of a pair of particles coupled to S and m_S is

$$\begin{aligned}P_{S,m_S}^i &= \sum_{\mu',\mu} C_{3,\mu',3,m_S-\mu'}^{S,m_S} C_{3,\mu,3,m_S-\mu}^{S,m_S} \\ &\quad \times \langle \varphi_{\mu',m_S-\mu'}^i | \varphi_{\mu,m_S-\mu}^i \rangle.\end{aligned} \tag{9}$$

One can prove from symmetry that $P_{S,m_S}^i = P_{S,-m_S}^i$ when $M(i) = 0$, and the $2S+1$ magnetic members P_{S,m_S}^i are equal to each other when $F(i) = 0$. Furthermore, we define

$$\mathfrak{P}_S^i = \sum_{m_S} P_{S,m_S}^i, \tag{10}$$

which is the probability that the spins of an arbitrary pair are coupled to S. In general, $\mathfrak{P}_S^i$ can provide information on the possible existence of two-body substructures as shown below.

As an example, let the normalized pair state be denoted as

$$\Psi_{\rm polar} = \gamma \tilde{P}_N [(\chi\chi)_0]^{N/2}, \tag{11}$$

where $\gamma = [N!(\frac{2}{7})^{N/2}(N/2)!\frac{(N+5)!!}{5!!}]^{-1/2}$ is the constant for normalization (refer to Appendix A). Since

$$\begin{aligned}\tilde{P}_N [(\chi\chi)_0]^{N/2} &= \sum_{S,m_S} [\chi(1)\chi(2)]_{S,m_S} B_{S,m_S} \\ &\quad \times \tilde{P}_{N-2} (\chi\chi)_{S,m_S} [(\chi\chi)_0]^{(N-4)/2},\end{aligned} \tag{12}$$

TABLE I. $\mathfrak{P}_S^{\text{polar}}$, the probability that a pair of particles in the polar state are coupled to S.

S	0	2	4	6
$\mathfrak{P}_S^{\text{polar}}$	$\frac{9(N+5)}{63(N-1)}$	$\frac{10(N-2)}{63(N-1)}$	$\frac{18(N-2)}{63(N-1)}$	$\frac{26(N-2)}{63(N-1)}$

where

$$B_{S,m_S} = N[\delta_{S,0}\delta_{m_S,0} + (-1)^{m_S}2(N/2-1)/7]. \quad (13)$$

By making use of the formulas in Appendix A, one can prove that all the P^i_{S,m_S} of the pair state are equal to $\frac{2(N-2)}{63(N-1)}$ with the only exception $P^i_{0,0} = \frac{9(N+5)}{63(N-1)}$. From these data, we obtain the $\mathfrak{P}^i_S$ of the pair state, denoted as $\mathfrak{P}_S^{\text{polar}}$, listed in Table I.

Note that, if the two particles are completely free (namely, their spin state is either $[\chi_\mu(1)\chi_\nu(2) + \chi_\mu(2)\chi_\nu(1)]/\sqrt{2}$ (if $\mu \neq \nu$) or $\chi_\mu(1)\chi_\nu(2)$ (if $\mu = \nu$), and the 28 choices of combination with $\mu \neq \nu$ and $\mu = \nu$ are considered as having equal weight), simply from the geometry, we will have $\mathfrak{P}_S^{\text{free}} = (2S+1)/\sum_{S'}(2S'+1)$, where S' covers 0, 2, 4, and 6. Therefore, $\mathfrak{P}_S^{\text{free}} = 0.036$, 0.179, 0.321, and 0.464 for $S = 0$, 2, 4, and 6, respectively, whereas for the pair state, $\mathfrak{P}_S^{\text{polar}} = 0.143$, 0.158, 0.286, and 0.413 when $N \to \infty$. Thus the ratios $\mathfrak{P}_S^{\text{polar}}/\mathfrak{P}_S^{\text{free}}$ are 4.0, 0.89, 0.89, and 0.89, where the ratio with $S = 0$ is remarkably large. Thus the big ratio is a signal of the importance of the singlet pairs.

The spin-spin correlation cannot be studied perfectly by MFT. The one-body and correlative probabilities together will help us to understand better the spin structures. In the fields of atomic and nuclear physics, it was found that the structures depend on N sensitively (the properties of an even-even nucleus are quite different from those of its neighboring even-odd nuclei). Since N is assumed to be small in this paper, the N dependence of condensates is also studied in the following.

III. POPULATIONS OF THE SPIN COMPONENTS OF THE GROUND STATES

We shall first study ^{52}Cr atoms as representative of spin-3 species. These atoms have $g_6 = 59.40$ meV Å^3, $g_4 = 0.5178g_6$, and $g_2 = -0.0625g_6$, while g_0 is unknown. In what follows $G_6 = g_6\int|\phi(\boldsymbol{r})|^4 d\boldsymbol{r}$ is considered as the unit of energy, and g_0 is variable. The one-body probabilities P^i_ν are first studied.

When N is even and $g_0 \to -\infty$, it has been proved that the ground state ψ_1 is exactly the pair state Ψ_{polar} written in Eq. (11) [7,14]. Obviously, the pair state has $F = 0$. It is a common feature that the P^i_ν of all the $F = 0$ states do not depend on ν due to the isotropism. Therefore, all of them are equal to $1/(2f+1) = 1/7$.

When N is odd and $g_0 \to -\infty$, ψ_1 is just the odd pair state written as

$$\Psi_{\text{odd polar},\mu} = \gamma'\tilde{P}_N\chi_\mu[(\chi\chi)_0]^{(N-1)/2}, \quad (14)$$

where $\gamma' = [N!(\frac{2}{7})^{(N-1)/2}(\frac{N-1}{2})!\frac{(N+6)!!}{7!!}]^{-1/2}$ is the constant of normalization (refer to Appendix A). Obviously, this state has $F = 3$. The associated one-body probability $P_\nu^{\text{odd polar},\mu}$ has the analytical form given in Table II (the derivation is given in Appendix B). For the case with a large N, it is shown in this table that $P_\nu^{\text{odd polar},\mu}$ depend on N very weakly. When the spin of the unpaired particle has $\mu = 0$, we know from Table II that the average population with $\nu = 0$ is the largest and is nearly three times as large as those with $\nu \neq 0$. When $\mu \neq 0$, the populations with $\nu = \mu$ and $-\mu$ are the largest two and they are nearly twice as large as those with $\nu \neq |\mu|$. On the other hand, it is recalled that $P_\nu^{\text{polar}} = 1/7$ which is greatly different from $P_\nu^{\text{odd polar},\mu}$. Thus, the populations of the spin components of a pair state will undergo a great change when a particle with a given μ is added into the state. This will happen even when N is very large. Such special even-odd dependence could be revealed by measuring the one-body probabilities if the polar state can be prepared.

TABLE II. One-body probability $P_\nu^{\text{odd polar},\mu}$, where μ is the spin component of the single (unpaired) particle in the odd polar state, and ν denotes the component of the particle under observation.

$\mu \neq 0$ $\nu = \mu$	$\mu \neq 0$ $\nu = -\mu$	$\mu \neq 0$ $\nu \neq \lvert\mu\rvert$	$\mu = 0$ $\nu = 0$	$\mu = 0$ $\nu \neq 0$
$\frac{2N+7}{9N}$	$\frac{2(N-1)}{9N}$	$\frac{N-1}{9N}$	$\frac{3(N+2)}{9N}$	$\frac{N-1}{9N}$

When g_0 increases from $-\infty$ but is still negative, ψ_1 with even N will still be more or less close to Ψ_{polar}. If the magnitudes of g_2, g_4, and g_6 were small, then ψ_1 would be closer. However, for realistic ^{52}Cr, g_4 and g_6 are not small. To see how much ψ_1 deviates from the pair state, $\langle\Psi_{\text{polar}}|\psi_1\rangle$ has been calculated. If $g_0/g_6 = -1$, -2, and -4, respectively, $\langle\Psi_{\text{polar}}|\psi_1\rangle = 0.838$, 0.936, and 0.981 when $N = 12$. This set of values will become 0.706, 0.841, and 0.937 when $N = 18$. Thus the deviation is not small unless g_0 is very negative.

For ^{52}Cr, the one-body probabilities P_3^1 of ψ_1 with $M = 0$ are plotted against g_0/g_6 in Fig. 2. The curves at the left side of Fig. 2(b) with even N are horizontal lines. They have the same value 1/7, implying that ψ_1 retains $F = 0$. The curves at the left side of Fig. 2(a) with odd N are close to each other, implying a weak dependence on N when N retains being odd. They are flat and have their values $\approx$0.038, which deviates explicitly from $P_3^{\text{odd polar},0} \approx 0.103$ given in Table II. It implies that the deviation between ψ_1 and $\Psi_{\text{odd polar},0}$ is not small when g_0 is close to -0.1.

By comparison of the right side of Fig. 2(a) with that of Fig. 2(b), the even-odd dependence is clearly shown. In addition, the curves with $N = 15$ and 18 are distinct. This implies that $N = 3K$ (K is an integer) is special. It is recalled that, for spin-2 condensates with a sufficiently negative g_2, the ground state is formed by the triplex $[(\eta\eta)_2\eta]_0$ [7,15,16]. The finding of the $3K$ dependence in spin-3 condensates is a hint that three-body substructures might exist as well.

In Fig. 2 the domain of g_0 is roughly divided into three regions. At the left side (region I) the curves depend on g_0 mildly, and the singlet pairs play an important role. At the right side (region III) the curves depend on g_0 also mildly, where three-body substructures might exist. In between (region II, roughly from $g_0/g_6 = 0$ to 0.1) the curves vary with g_0 very swiftly, implying a swift change in spin structure. In addition,

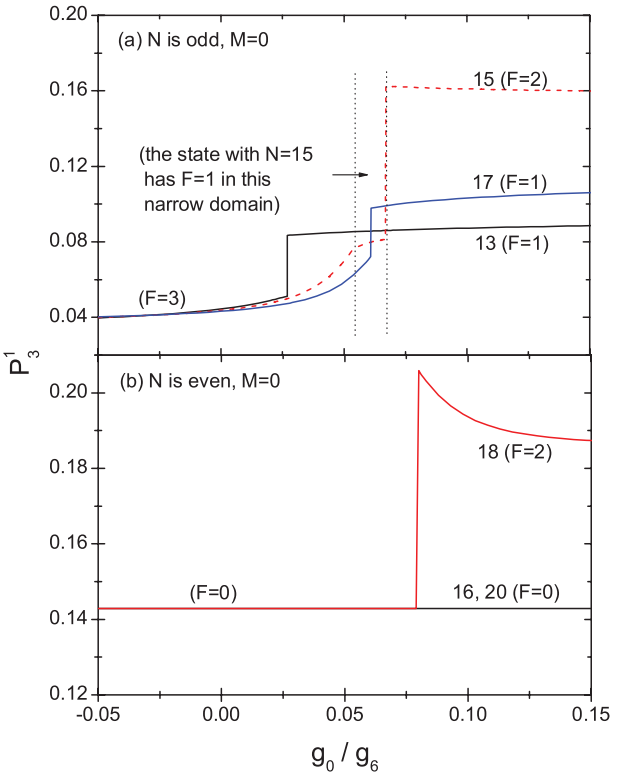

FIG. 2. (Color online) P^1_3 of the ground state ψ_1 with $M = 0$ against g_0/g_6. g_2, g_4, and g_6 are given at the experimental values of ^{52}Cr. The values of N are marked by the curves. The total spin F of ψ_1 is given inside the parentheses; it will jump whenever g_0 crosses a critical point. Note that NP^i_ν is the average population of the ν component of the ψ_i state.

a critical point may appear in this region (e.g., $g_0/g_6 = 0.079$ is a critical point when $N = 18$ and $M = 0$), where P^1_3 varies abruptly. Once g_0 crosses a critical point F might change suddenly, implying a transition of spin structure.

Incidentally, according to the MFT, there are also three regions. The phases of the ground state in these regions are named maximum polar (A), collinear polar (B), and biaxial nematic (C) in Ref. [9] when g_0 varies from negative to positive, The associated spinors are $(1,0,0,0,0,0,1)$, $(a,0,be^{i\delta},0,be^{i\delta},0,a)$, and $(a,0,b,0,c,0,d)$. The critical point between A and B is $g_0/g_6 = 0.079$. In Ref. [10], the three phases are named the polar phase, the mixed phase, and the cyclic phase. The associated spinors are $(\cos\theta,0,0,0,0,0,\sin\theta)$, $(0,a,0,b,0,a,0)$, and $(a,0,b,0,b,0,a)$, respectively (the third spinor may mix with the second spinor in the mixed phase). In this paper a different language is used so that the structures can be understood via a different path.

IV. CORRELATIVE PROBABILITIES OF THE GROUND STATES

The curves at the left side of Fig. 2(b) are horizontal until the critical point. However, the spin structures are in fact changing in this broad region. This example demonstrates that the information provided by the one-body probabilities is not sufficient. Therefore, the correlative probabilities are further

TABLE III. $P^{\text{polar}}_{\mu\nu}$, the correlative probabilities of the polar state.

(μ,ν)	$(0,0)$	$(\mu \neq 0, -\mu)$	$(\mu \neq 0,\mu)$	Otherwise
$P^{\text{polar}}_{\mu\nu}$	$\frac{3(N+1)}{63(N-1)}$	$\frac{2N+5}{63(N-1)}$	$\frac{2(N-2)}{63(N-1)}$	$\frac{N-2}{63(N-1)}$

studied. First, for the pair state, the probabilities $P^{\text{polar}}_{\mu\nu}$ are given in Table III (the derivation is referred to Appendix C).

It is shown that $P^{\text{polar}}_{\mu\nu}$ are all nearly independent of N unless N is small. The largest component is $P^{\text{polar}}_{0,0}$. The probabilities of being spin parallel and spin antiparallel, i.e., $P^{\text{polar}}_{\mu,\mu}$ and $P^{\text{polar}}_{\mu,-\mu}$, are equal when $N \to \infty$.

Examples of $P^1_{\mu\nu}$ of ψ_1 with even N are given in Fig. 3. The curves with $N = 18$ are also distinct and jump up suddenly at the critical point. The jump is accompanied by a change of the total spin F from 0 to 2, implying a transition. Since the curves vary rapidly in the neighborhood of the critical point, strong adjustment in structure happens right before and after the transition. The strong adjustment in the neighborhood of the critical point is a notable phenomenon. The curves with $N = 16$ and 20 are similar to each other. In particular, they retain their $F = 0$ and accordingly they do not have the sudden jump. The critical point will appear whenever N is a multiple of 3 and will shift a little to the left when N becomes larger (e.g., they appear at $g_0/g_6 = 0.252$, 0.079, and 0.075, respectively, when $N = 12$, 18, and 24). The shift will be very small if $\Delta N/N$ is small.

The curves of $P^1_{\mu\nu}$ with odd N are in general very different from those with even N. They also exhibit the $3K$ dependence and contain critical points in region II. For an example, there

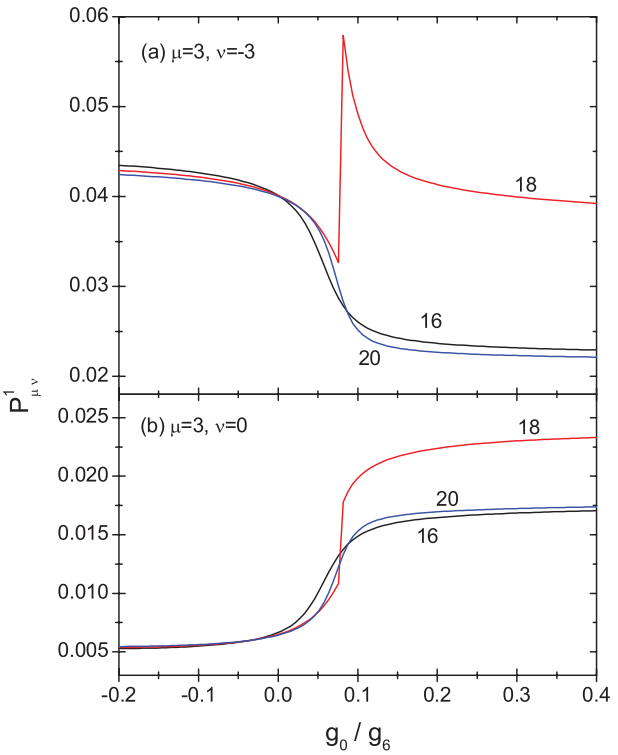

FIG. 3. (Color online) $P^1_{\mu\nu}$ of the ground state ψ_1 of ^{52}Cr against g_0/g_6. N is even and is marked by the side of each curve, and $M = 0$.

TABLE IV. $\mathcal{P}_S^1/\mathcal{P}_S^{\rm free}$ of the ground states of ^{52}Cr with $N = 18$, $M = 0$, and g_0 at five presumed values.

$\mathcal{P}_S^1/\mathcal{P}_S^{\rm free}$	$S = 0$	$S = 2$	$S = 4$	$S = 6$
$g_0/g_6 = -0.2$	4.58	1.78	0.14	1.02
$g_0/g_6 = 0.07$	2.44	1.90	0.50	0.89
$g_0/g_6 = 0.09$	0.75	1.92	0.83	0.78
$g_0/g_6 = 0.5$	0.04	1.88	1.02	0.72
$g_0/g_6 = 1$	0.01	1.87	1.04	0.72

are two critical points appearing at $g_0/g_6 = 0.058$ and 0.067 when $N = 15$ and $M = 0$. Accordingly, F jumps from 3 to 1 and then to 2 when g_0 increases.

V. MIXING OF $S = 0$ AND 2 PAIRS

Let us study $\mathcal{P}_S^i$, the probabilities of the spins of two particles being coupled to S. $\mathcal{P}_S^1$ of ψ_1 is close to $\mathcal{P}_S^{\rm polar}$ when N is even and $g_0 \to -\infty$. When g_0 is not so negative, examples of $\mathcal{P}_S^1/\mathcal{P}_S^{\rm free}$ are listed in Table IV, where $g_0/g_6 = -0.2$ is in region I, 0.07 and 0.09 are in region II and lying by the left and right sides of the critical point (at 0.079), and 0.5 and 1 are in region III.

We found that $\mathcal{P}_0^1/\mathcal{P}_0^{\rm free}$ is quite large when $g_0/g_6 = -0.2$. This implies a preference for the singlet pairs. However, the four ratios $\mathcal{P}_S^1/\mathcal{P}_S^{\rm free}$ as a whole deviate explicitly from $\mathcal{P}_S^{\rm polar}/\mathcal{P}_S^{\rm free}$. Therefore ψ_1 is quite different from that of the pair state. When g_0 increases further, the ratio with $S = 0$ keeps on decreasing. In particular, it decreases very rapidly when g_0 is passing through the critical point. On the other hand, the probability of the $S = 2$ pair remains larger. In particular, it becomes the largest when g_0 is larger than the critical value. Therefore, the dominance of the singlet pairs is gradually replaced by dominance of the $S = 2$ pairs. Hence, for N even, we define a set of basis functions formed by the two kinds of pairs as

$$\Phi_j^{\rm pairs} = \beta_j \tilde{P}_N\{[(\chi\chi)_0]^{K_p}[(\chi\chi)_{2,2}]^{K_2} \cdots [(\chi\chi)_{2,-2}]^{K_{-2}}\}, \quad (15)$$

where j denotes the set $(K_p, K_2, \ldots, K_{-2})$ of non-negative integers, and their sum is $N/2$. β_j provides the normalization. The space expanded by $\Phi_j^{\rm pairs}$ is much smaller than that expanded by the Fock state. For example, if $N = 18$ and $M = 0$, the numbers of Fock states and $\Phi_j^{\rm pairs}$ are 3486 and 148, respectively. The eigenstates can be approximately expanded as

$$\psi_i \approx \sum_j b_j \Phi_j^{\rm pairs} \equiv \tilde{\psi}_i, \quad (16)$$

where b_j can be obtained via a diagonalization of $H_{\rm mod}$ in the much smaller space (note that $\Phi_j^{\rm pairs}$ are not exactly orthogonal to each other).

The overlap $|\langle\tilde{\psi}_1|\psi_1\rangle|$ of the approximate and exact ground states against g_0 is plotted in Fig. 4. The solid curve ($N = 18$) is extremely close to 1 when g_0 is below the critical point. This confirms the physical picture that both the $S = 0$ and 2 pairs are building blocks. However, the solid curve has a sudden fall at the critical point. Thus the picture is spoiled when g_0 is larger, and we have to look for other structures. The dashed curve ($N = 16$) represents the case without a transition, where a swift descent replaces the sudden fall.

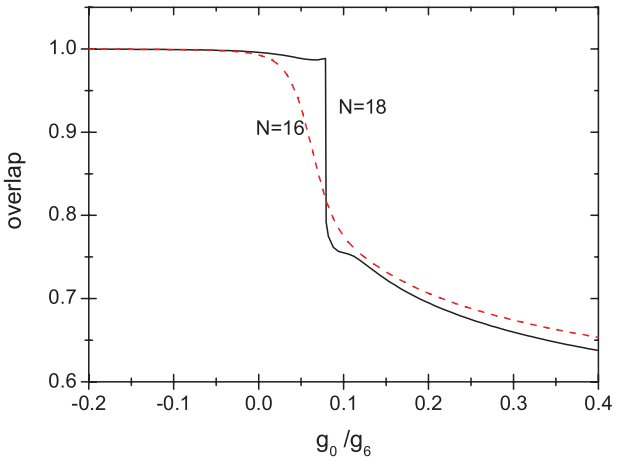

FIG. 4. (Color online) The overlap $|\langle\tilde{\psi}_1|\psi_1\rangle|$ of the exact ground state ψ_1 of ^{52}Cr (the one expanded in Fock states) and the corresponding approximate state $\tilde{\psi}_1$ (using the $S = 0$ and 2 pairs as building blocks) against g_0. $N = 18$ (solid) and 16 (dashed), and $M = 0$.

VI. CANDIDATES FOR THREE-BODY SUBSTRUCTURES AND THE TRIPLEX STATES

In order to see whether three-body substructures exist in region III, let us first analyze a three-body spin-3 system. Let

$$\xi_{\sigma\lambda m_\lambda} = \beta_{\sigma\lambda}\tilde{P}_3((\chi\chi)_\sigma\chi)_{\lambda m_\lambda} \quad (17)$$

be a spin state of the three-boson system, where two spins are first coupled to σ. Then they are coupled to λ and m_λ, the total spin and its Z component. $\beta_{\sigma\lambda}$ provides the normalization. In total there are eight independent $\xi_{\sigma\lambda}$ (the subscript m_λ can be neglected) given in the top row of Table V. Those not listed in the table are linear combinations of them (e.g., $\xi_{2,1} \equiv \xi_{4,1}$). Each of them represents a specific three-body spin structure. Incidentally, these eight $\xi_{\sigma\lambda}$ are exactly orthogonal to each other except for $\xi_{2,3}$ and $\xi_{4,3}$.

By extracting two particles from $\xi_{\sigma\lambda}$, one can define and calculate the probabilities $p_S^{\sigma\lambda}$ that the two spins are coupled to S. They are given in Table V. If a three-body substructure is a basic constituent, it must be very stable. Since $p_6^{\sigma\lambda}$ of $\xi_{2,1}$ and $\xi_{4,3}$ are zero or extremely small, the repulsion arising from g_6 can be avoided in them. Therefore $\xi_{2,1}$ and $\xi_{4,3}$ will be relatively more stable when g_6 is more positive than the others. In a further competition between $\xi_{2,1}$ and $\xi_{4,3}$, if g_4 is negative and g_2 is positive, $\xi_{4,3}$ will be more stable due to having a large $p_4^{\sigma\lambda}$. On the contrary, if g_4 is positive and g_2 is negative, $\xi_{2,1}$ will be more stable.

To evaluate the importance of a substructure quantitatively, from an N-body spin state ψ_i, we define $\Phi^i_{\sigma\lambda m_\lambda} \equiv \langle\xi_{\sigma\lambda m_\lambda}|\psi_i\rangle$, which is an $(N-3)$-body spin state. Then, for three arbitrary particles in ψ_i, the probability that they form the $\xi_{\sigma\lambda}$ substructure is $Q^i_{\sigma\lambda} \equiv \sum_{m_\lambda}\langle\Phi^i_{\sigma\lambda m_\lambda}|\Phi^i_{\sigma\lambda m_\lambda}\rangle$. Note that $Q^i_{\sigma\lambda}$ depends on the total spin of ψ_i, $F(i)$, but not on $M(i)$ because of the summation over m_λ. If the particle correlation is removed, the

TABLE V. The probabilities $p_S^{\sigma\lambda}$ that a pair of particles are coupled to S in the three-body states $\xi_{\sigma\lambda}$.

σ,λ	2,1	2,3	4,3	2,4	2,5	4,6	4,7	6,9
$p_0^{\sigma\lambda}$	0	0.094	0.108	0	0	0	0	0
$p_2^{\sigma\lambda}$	0.524	0.484	0.135	0.611	0.413	0	0	0
$p_4^{\sigma\lambda}$	0.476	0.211	0.753	0.061	0.234	0.727	0.515	0
$p_6^{\sigma\lambda}$	0	0.211	0.003	0.328	0.353	0.273	0.485	1

corresponding probability will be $Q_{\sigma\lambda}^{\rm free} \equiv \frac{2\lambda+1}{\sum_{\lambda'}(2\lambda'+1)}$ where the summation over λ' covers the eight states listed in Table V (i.e., $\lambda' = 1$, 3, 3, 4, 5, 6, 7, and 9, where $\lambda' = 3$ should be counted twice). Then, we define the ratio $\rho_{\sigma\lambda}^i \equiv Q_{\sigma\lambda}^i / Q_{\sigma\lambda}^{\rm free}$. If this quantity is much larger than 1, the substructure $\xi_{\sigma\lambda}$ is much preferred.

As an example, we leave ^{52}Cr for a while and assume that $g_6 = 1$, $g_4 = -1$, $g_2 = 0.2$, and $g_0 = -0.2$. Since g_4 has been chosen to be rather negative, $\xi_{4,3}$ is expected to be important. To verify, the ratios denoted as $\rho_{\sigma\lambda}^1(A)$ for the ground state with $N = 18$ are listed in Table VI.

It is shown that $\rho_{4,3}^1(A)$ is particularly large. Therefore $\xi_{4,3}$ is highly preferred by the ground state as expected, and one might further expect that the triplex $\xi_{4,3}$ might play a role as a building block. To clarify, we introduce a set of basis functions for the case with $N = 3K$ as

$$\Phi_j^{\rm triplex} = \beta_j' \tilde{P}_N \{[\xi_{4,3,3}]^{K_3}[\xi_{4,3,2}]^{K_2} \cdots [\xi_{4,3,-3}]^{K_{-3}}\}, \quad (18)$$

in which $\sum_\mu K_\mu = N/3$ and $\sum_\mu \mu K_\mu = M$. For $N = 18$ and $M = 0$, there are totally 58 basis functions, much smaller than the number 3486 of the Fock-states. After a diagonalization of $H_{\rm mod}$ in the 58-dimensional space, we obtain the approximate eigenstates $\psi_i^{\rm triplex} = \sum_j d_j \Phi_j^{\rm triplex}$ to be compared with the exact eigenstates ψ_i. It turns out that $|\langle \psi_i^{\rm triplex} | \psi_i \rangle| = 0.999$, 0.996, and 0.990 for $i = 1$, 2, and 3, respectively [they are the three lowest states having $F(i) = 0$, 4, and 6, respectively]. Such a great overlap confirms that, as in the spin-2 condensates, the triplex structure exists also in spin-3 condensates. However, the triplex of spin-2 condensates has $\lambda = 0$; thus there is only one kind of building block, whereas the triplex now has $\lambda = 3$ and therefore has $2\lambda + 1 = 7$ kinds of building block. This leads to complexity.

We go back to the case of ^{52}Cr atoms. Let g_2, g_4, and g_6 be set at the experimental values and g_0/g_6 at some presumed positive values (i.e., only g_2 is negative). Since $\xi_{4,3}$ has a large $P_4^{\sigma\lambda}$, it is no longer superior. Instead, $\xi_{2,4}$ might be important due to having a very small $P_4^{\sigma\lambda}$. When $g_0/g_6 = 0.5$, the ratios denoted as $\rho_{\sigma\lambda}^1(B)$ have been calculated and they are listed in the bottom row of Table VI, where both $\rho_{2,1}^i$ and $\rho_{2,4}^i$ are large due to having a larger $P_2^{\sigma\lambda}$. Therefore, in total the 12 $\xi_{2,1,m_\lambda}$ and $\xi_{2,4,m_\lambda}$ are used as building blocks, and we define another set of basis functions as

$$\Phi_j^{\rm tri,tri} = \beta_j'' \tilde{P}_N \left\{ \left(\prod_{m_a} [\xi_{2,1,m_a}]^{K_{a,m_a}} \right) \times \left(\prod_{m_b} [\xi_{2,4,m_b}]^{K_{b,m_b}} \right) \right\}, \quad (19)$$

where m_a runs from -1 to 1, m_b from -4 to 4, $\sum_{m_a} K_{a,m_a} + \sum_{m_b} K_{b,m_b} = N/3$, and $\sum_{m_a} m_a K_{a,m_a} + \sum_{m_b} m_b K_{b,m_b} = M$. The number of $\Phi_j^{\rm tri,tri}$ is 758 when $N = 18$ and $M = 0$. However, only 615 of them are linearly independent. With $\Phi_j^{\rm tri,tri}$, we have calculated the approximate eigenstate $\psi_{i'}^{\rm tri,tri}$ at five values of g_0/g_6 (where two negative values are included for a comparison), and the overlaps $|\langle \psi_{i'}^{\rm tri,tri} | \psi_i \rangle|$ are listed in Table VII. Recall that $g_0/g_6 = 0.079$ is a critical point. Once g_0/g_6 is larger than the critical point, the overlaps are very close to 1. Thus the picture of triplexes is theoretically confirmed, whereas this picture is not well established when g_0 is smaller than the critical point, where the $S = 0$ and 2 pairs are dominant.

VII. FINAL REMARKS

Instead of using the MFT, a language from few-body theory is used in this paper. We have shown theoretically the existence of stable two- and three-body structures as building blocks in small spin-3 condensates. The ratios $\mathfrak{P}_S^i / \mathfrak{P}_S^{\rm free}$ and $Q_{\sigma\lambda}^i / Q_{\sigma\lambda}^{\rm free} \equiv \rho_{\sigma\lambda}^i$ defined in this paper are important in the search for these basic constituents. The reason leading to the appearance of these constituents is explained based on the features of the interaction, whereas, in the MFT, the physics underlying the appearance of a specific spinor is not easy to clarify.

The calculation in this paper concerns only small spin-3 condensates ($N \leqslant 24$). For spin-2 condensates, it has been proved theoretically that the fact that pairs and triplexes appear as building blocks does not depend on N (In fact, the picture of the triplexes would become even clearer when $N \to \infty$ [7]). It has also been proved that the existence of the pairs in spin-3 condensates does not depend on N [7,14]. Thus the existence of triplexes as building blocks in large spin-3 condensates is very probable; nonetheless it deserves further study.

TABLE VI. $\rho_{\sigma\lambda}^1$ of the ground state with $N = 18$. The parameters of interaction associated with the cases A and B are given in the text.

σ,λ	2,1	2,3	4,3	2,4	2,5	4,6	4,7	6,9
$\rho_{\sigma\lambda}^1(A)$	0.099	0.119	4.425	0.032	0.069	1.813	0.967	0.204
$\rho_{\sigma\lambda}^1(B)$	3.485	1.180	1.011	2.399	1.231	0.728	0.752	0.390

TABLE VII. The overlap $|\langle\psi_{i'}^{\mathrm{tri,tri}}|\psi_i\rangle|$, where $\psi_{i'}^{\mathrm{tri,tri}}$ is the triplex state formed by using $\xi_{2,1,m_\lambda}$ and $\xi_{2,4,m_\lambda}$ as building blocks. $N = 18$ and 12 and $M = 0$ are given. The parameters g_2, g_4, and g_6 are from the experimental data of ^{52}Cr, while g_0/g_6 is denoted as g' and given at five values. i' is so chosen that, if ψ_i is the kth eigenstate of the series with $F = F(i)$, then $\psi_{i'}^{\mathrm{tri,tri}}$ is also the kth state of the series of triplex states with $F(i') = F(i)$. $F(i)$ are given in parentheses following the overlaps.

	$g' = -1$	$g' = -0.5$	$g' = 0.1$	$g' = 0.5$	$g' = 1$
$\lvert\langle\psi_{i'_1}^{\mathrm{tri,tri}}\rvert\psi_1\rangle\rvert_{N=18}$	0.908 (0)	0.958 (0)	1.000 (2)	0.998 (2)	0.983 (2)
$\lvert\langle\psi_{i'_2}^{\mathrm{tri,tri}}\rvert\psi_2\rangle\rvert_{N=18}$	0.859 (2)	0.935 (2)	1.000 (0)	0.998 (2)	0.998 (4)
$\lvert\langle\psi_{i'_3}^{\mathrm{tri,tri}}\rvert\psi_3\rangle\rvert_{N=18}$	0.915 (4)	0.959 (4)	1.000 (2)	0.999 (0)	0.981 (2)
$\lvert\langle\psi_{i'_1}^{\mathrm{tri,tri}}\rvert\psi_1\rangle\rvert_{N=12}$	0.861 (0)	0.934 (0)	1.000 (0)	0.997 (2)	0.988 (2)
$\lvert\langle\psi_{i'_2}^{\mathrm{tri,tri}}\rvert\psi_2\rangle\rvert_{N=12}$	0.756 (2)	0.869 (2)	1.000 (2)	0.999 (0)	0.998 (0)
$\lvert\langle\psi_{i'_3}^{\mathrm{tri,tri}}\rvert\psi_3\rangle\rvert_{N=12}$	0.813 (4)	0.905 (4)	1.000 (3)	0.999 (1)	0.998 (1)

ACKNOWLEDGMENT

The support from the NSFC under Grant No. 10874249 is appreciated.

APPENDIX A: ITERATION RELATIONS

For the pair state and odd-pair state the following equations relating an N-body and an $(N-2)$-body systems are very useful:

$$\begin{aligned}\mathcal{N}_0^{(N)} &\equiv \langle\tilde{P}_N[(\chi\chi)_0]^{N/2}|\tilde{P}_N[(\chi\chi)_0]^{N/2}\rangle,\\ &= \tfrac{1}{7}N^2(N-1)(N+5)\mathcal{N}_0^{(N-2)},\end{aligned} \tag{A1}$$

$$\begin{aligned}\mathcal{N}_{\mathrm{odd}}^{(N)} &\equiv \langle\tilde{P}_N\chi_\mu[(\chi\chi)_0]^{(N-1)/2}|\tilde{P}_N\chi_\mu[(\chi\chi)_0]^{(N-1)/2}\rangle\\ &= \tfrac{1}{7}N(N-1)^2(N+6)\mathcal{N}_{\mathrm{odd}}^{(N-2)},\end{aligned} \tag{A2}$$

$$\begin{aligned}\mathcal{N}_{S,m_S}^{(N)} &\equiv \langle\tilde{P}_N(\chi\chi)_{Sm_S}[(\chi\chi)_0]^{(N-2)/2}|\tilde{P}_N(\chi\chi)_{Sm_S}\\ &\quad\times[(\chi\chi)_0]^{(N-2)/2}\rangle\\ &= \tfrac{1}{7}N(N-1)(N-2)(N+7)\mathcal{N}_{S,m_S}^{(N-2)},\end{aligned} \tag{A3}$$

where $\tilde{P}_N$ denotes a summation over the $N!$ permutation terms. Equation (A3) holds only if $S \neq 0$ [if $S = 0$, then Eq. (A1) should be used]. By making use of these equations, related matrix elements can be derived via iteration. For example, the constant of normalization γ can be obtained from Eq. (A1) and γ' from Eq. (A2).

APPENDIX B: THE ONE-BODY PROBABILITIES OF ODD-PAIR-STATES

One can extract a particle (say, particle 1) from an odd-pair state as

$$\begin{aligned}\tilde{P}_N\chi_\mu[(\chi\chi)_0]^K &= \sum_\nu \chi_\nu(1)\Big\{\delta_{\mu,\nu}\tilde{P}_{N-1}[(\chi\chi)_0]^K\\ &\quad-(N-1)\frac{(-1)^\nu}{\sqrt{7}}\sum_S C_{3\mu,3,-\nu}^{S,\mu-\nu}\\ &\quad\times\tilde{P}_{N-1}(\chi\chi)_{S,\mu-\nu}[(\chi\chi)_0]^{K-1}\Big\},\end{aligned} \tag{B1}$$

where $K = (N-1)/2$, the Clebsch-Gordan coefficients have been introduced, and only even S are included in the summation. Then, from the definition of the one-body probability, we have

$$\begin{aligned}P_\nu^{\text{odd polar}} &= \delta_{\mu,\nu}\frac{4K+7}{7}\frac{\mathcal{N}_0^{(N-1)}}{\mathcal{N}_{\mathrm{odd}}^{(N)}}\\ &\quad+\frac{4K^2}{7}\sum_S\left(C_{3\mu,3,-\nu}^{S,\mu-\nu}\right)^2\frac{\mathcal{N}_{S,\mu-\nu}^{(N-1)}}{\mathcal{N}_{\mathrm{odd}}^{(N)}}.\end{aligned} \tag{B2}$$

We mention that the expression of $\mathcal{N}_{S,\mu-\nu}^{(N-1)}$ depends on whether S is zero or nonzero. With this in mind, after a simplification, Eq. (B2) leads to the expressions given in the text.

APPENDIX C: THE CORRELATIVE PROBABILITIES OF PAIR STATES

One can extract two particles (say, 1 and 2) from a pair state as

$$\begin{aligned}&\tilde{P}_N[(\chi\chi)_0]^{N/2}\\ &= N\sum_{\mu\nu}\chi_\mu(1)\chi_\nu(2)\Big\{\delta_{\mu,-\nu}C_{3\mu,3\nu}^{0,0}\tilde{P}_{N-2}[(\chi\chi)_0]^{(N-2)/2}\\ &\quad+(N-2)\sum_S(2S+1)U\begin{pmatrix}3&3&0\\3&3&0\\S&S&0\end{pmatrix}C_{S,\mu+\nu,S,-\mu-\nu}^{0,0}\\ &\quad\times C_{3\mu,3\nu}^{S,\mu+\nu}\tilde{P}_{N-2}(\chi\chi)_{S,-\mu-\nu}[(\chi\chi)_0]^{(N-4)/2}\Big\},\end{aligned} \tag{C1}$$

where the Clebsch-Gordan and $9j$ coefficients have been introduced, and only even S are included in the summation. Then, from the definition of the correlative probability, we have

$$\begin{aligned}P_{\mu\nu}^{\text{polar}} &= \left(\frac{N}{7}\right)^2\Bigg[\delta_{\mu,-\nu}(2N+3)\frac{\mathcal{N}_0^{(N-2)}}{\mathcal{N}_0^{(N)}}\\ &\quad+(N-2)^2\sum_S\left(C_{3\mu,3\nu}^{S,\mu+\nu}\right)^2\frac{\mathcal{N}_{S,\mu+\nu}^{(N-2)}}{\mathcal{N}_0^{(N)}}\Bigg].\end{aligned} \tag{C2}$$

After a simplification, Eq. (C2) leads to the expressions given in the text.

[1] E. W. Schmid, Nucl. Phys. A **416**, 347c (1984); **416**, 379c (1984).
[2] N. D. Cook, *Models of the Atomic Nucleus*, 2nd ed. (Springer, Berlin, 2010).
[3] L. N. Cooper, Phys. Rev. **104**, 1189 (1956).
[4] A. M. Kadin, J. Supercond. Novel Magn. **20**, 285 (2005).
[5] C. K. Law, H. Pu, and N. P. Bigelow, Phys. Rev. Lett. **81**, 5257 (1998).
[6] C. G. Bao and Z. B. Li, Phys. Rev. A **70**, 043620 (2004).
[7] P. V. Isacker and S. Heinze, J. Phys. A **40**, 14811 (2007).
[8] J. Katriel, J. Mol. Struct.: THEOCHEM **547**, 1 (2001).
[9] R. B. Diener and T. L. Ho, Phys. Rev. Lett. **96**, 190405 (2006).
[10] L. Santos and T. Pfau, Phys. Rev. Lett. **96**, 190404 (2006).
[11] H. Mäkelä and K.-A. Suominen, Phys. Rev. A **75**, 033610 (2007).
[12] The suppression of $V_{\rm dd}$ in a strong isotropic trap can also be seen under the framework of MFT. In this theory, the effect of $V_{\rm dd}$ is embodied by the factor $c_d\Gamma_0$, where c_d is the strength and is usually small ($c_d = 0.0036g_6$ for ^{52}Cr), and $\Gamma_0 = \int d\boldsymbol{R}d\boldsymbol{r}\ |\phi(\boldsymbol{r}_1)|^2|\phi(\boldsymbol{r}_2)|^2\ Y_{20}(\hat{\boldsymbol{r}})/\ |\boldsymbol{r}|^3$, where $\phi(\boldsymbol{r}_i)$ is the spatial wave function of the ith particle, $\boldsymbol{R} = (\boldsymbol{r}_1 + \boldsymbol{r}_2)/2$, and $\boldsymbol{r} = \boldsymbol{r}_1 - \boldsymbol{r}_2$ [10]. A part of the integrand can be in general expanded as $|\phi(\boldsymbol{r}_1)|^2|\phi(\boldsymbol{r}_2)|^2 = \sum_{l_a,l_b,L} B_{l_a,l_b,L}(R,r)(Y_{l_a}(\hat{\boldsymbol{R}})Y_{l_b}(\hat{\boldsymbol{r}}))_L$, where l_a and l_b denote the partial waves and they are coupled to L. Since ϕ is close to isotropic when the trap is strong, the $L \neq 0$ terms can be neglected. This leads to $\Gamma_0 = 0$. Thus the effect of $V_{\rm dd}$ is suppressed.
[13] M. S. Chang, Q. Qin, W. X. Zhang, L. You, and M. S. Chapman, Nat. Phys. **1**, 111 (2005).
[14] C. G. Bao, Few-Body Syst. **46**, 87 (2009).
[15] M. Ueda and M. Koashi, Phys. Rev. A **65**, 063602 (2002).
[16] Y. Z. He and C. G. Bao, Phys. Rev. A **83**, 033622 (2011).